

# Design and Analysis of Multiple-Beam Reflector Antennas

**Sudhakar K. Rao**

Hughes Space and Communications  
 Loc. SC, Building S12, Mail Stop V 348  
 1950 E. Imperial Highway, PO Box 92919  
 Los Angeles, CA 90009  
 Tel: +1 (310) 662-7241  
 Fax: +1 (310) 416-5656  
 E-mail: skrao@mail.hac.com

**Keywords:** multiple beam antennas; shaped beam antennas; reflector antennas; offset reflector antennas; antenna radiation patterns; aperture antennas; satellite communication; space vehicle communication; lens antennas

## 1. Abstract

Simplified design and analysis equations are presented for multiple-beam reflector antennas based on the Gaussian-beam analysis of the primary and secondary patterns. The derived equations are useful for the quick design and performance analysis in terms of the coverage-area directivity and the inter-beam isolation of multiple-beam antenna systems. Results of the analysis given in this paper agree well with rigorous computations based on physical-optics analysis of the reflector-antenna radiation patterns. Extension of the analysis to multiple-beam lens antennas, and to shaped/contoured-beam antennas, is also presented.

## 2. Introduction

Multiple-beam antennas (MBA) are currently being used to provide the downlink and uplink coverage for mobile communication satellites, direct broadcast satellites, and personal communication satellites. These antennas typically provide contiguous coverage over a specified field-of-view by using high-gain overlapping spot beams. For effective utilization of the frequency spectrum of these satellite systems, the frequency is reused on a number of beams. This is done by dividing the available bandwidth into a number of sub-bands, typically using either a three-cell or a four-cell frequency-reuse scheme. The design objectives are to maximize the minimum-coverage-area directivity and to maximize the co-polar isolation ( $C/I$ ) among the beams reusing the frequency.

Antenna designs that are suitable and most often used for multiple-beam antennas are: (a) a single-aperture design with a single element per beam, (b) a single-aperture design with overlapping feed clusters, (c) direct radiating arrays, and (d) a multiple-aperture design with a single element per beam. The apertures are usually offset-parabolic reflector antennas and could also be dielectric lenses. Design (a) requires small horns (about  $1.0\lambda$  diameter) to be used, in order to achieve high adjacent beam overlap, which results in gain values that are 2 to 3 dB lower than what could be achieved using an optimal size horn [1, 2]. Design (b) requires a low-level beam-forming network to provide the element sharing among a number of beams (usually three or seven), and

beam-combining functions. Although design (b) provides good gain and  $C/I$  performance, the amplifiers operate in a multi-carrier environment, which reduces the efficiency of the amplifiers. Design (c) is similar to design (b), except that each beam utilizes all the elements of the array.

The multiple-aperture design with a single element per beam (design d) typically employs three or four independent apertures, as shown in Figure 1. Adjacent beams are generated from different apertures, forming an interleaved spot-beam coverage on the ground. The closest spacing between adjacent beams from the same aperture can be increased from  $\theta$  to  $1.732\theta$  for a three-aperture design, and to  $2.0\theta$  for a four-aperture design, where  $\theta$  is the center-to-center spacing between adjacent beams of the multiple-beam coverage. The larger beam spacing allows a proportionate increase in the horn size, which, in turn, improves the antenna gain through reduced spillover loss. The scope of this paper is

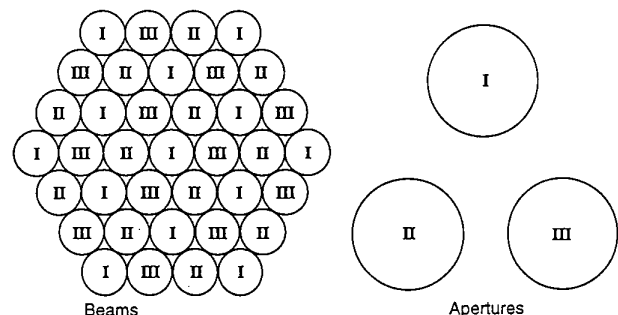


Figure 1a. A three-aperture system multiple-beam antenna design. I, II, and III represent the frequency cells.

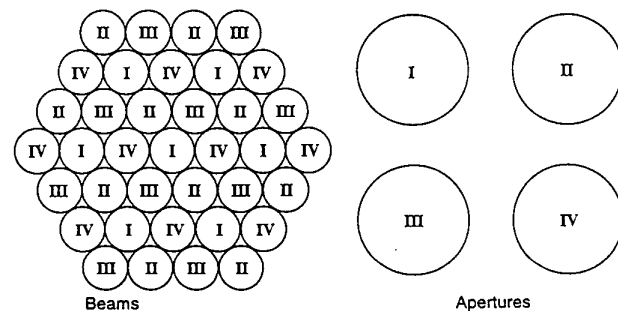


Figure 1b. A four-aperture system multiple-beam antenna design. I, II, III, and IV represent the frequency cells.

mostly limited to multiple-aperture designs where the apertures are offset-parabolic reflectors.

Design and performance analysis of the MBAs is quite tedious. It requires several iterations of first computing the radiation patterns of reflector antennas for all beams, using the Physical Optics (PO) method, and then performing the minimum-coverage-area directivity and the  $C/I$  evaluations for each beam. The whole process typically takes a few weeks to arrive at an optimal MBA design. The objective of this paper is to present a simplified analysis for the multiple-beam reflector-antenna system, such that the complete design and analysis can be performed very efficiently within a few minutes, using hand calculators. The analysis is based on approximating the primary as well as secondary patterns as Gaussian beams, and deriving simplified equations for the MBA design and performance evaluation. The results of the analysis presented in this paper agree well with those computed using the PO analysis of reflector antennas. The design equations provide a very good starting solution for the MBA design, and the PO analysis can then be used for the final design optimization and evaluation of the MBA performance. It is also shown that the analysis presented can easily be extended to lens MBAs, and to shaped- or contoured-beam antennas.

### 3. Design and analysis

The design of a multiple-beam antenna depends on the beam size, which is related to the minimum-coverage-area directivity requirement. For MBAs with uniform-size beams, arranged in a hexagonal grid fashion, the minimum directivity occurs at the triple beam crossover of the three adjacent beams, as shown in Figure 2a. Typical beam overlaps used for MBA designs are 3 dB for two adjacent beams, and 4 dB for three adjacent beams. The optimum overlap level depends on the minimum-coverage directivity, required co-polar isolation ( $C/I$ ) among reuse beams, and the frequency-reuse scheme (three-cell, four-cell, etc.). The spacing between adjacent-beam centers,  $\theta$ , determines the number of beams for a given coverage, and the maximum feed size that could be used for the reflectors. For the hexagonal-grid layout of the beams, as shown in Figure 2a,  $\theta_s$  is given as

$$\theta_s = 0.866\theta_0, \quad (1)$$

where  $\theta_0$  is the beam diameter at the triple beam crossover. The minimum number of beams,  $N_{min}$ , for a given coverage area is given approximately as

$$N_{min} = \text{Coverage Area} / (0.866\theta_s^2). \quad (2)$$

The denominator of Equation (2) represents the area of the hexagonal cell associated with each beam. The coverage area (in square degrees) includes the pointing error of the satellite. The actual number of beams,  $N_A$ , is typically 20% larger than  $N_{min}$  for an efficient layout of the beams over the coverage, such that the triple beam crossover levels for outer beams occur at the edge of the coverage. For three-reflector (using the three-cell reuse scheme) and four-reflector (using the four-cell reuse scheme) antenna systems, the closest spacings between beam centers reusing the same frequency are given respectively by

$$\theta_c^3 = 1.732\theta_s \quad (3)$$

$$\theta_c^4 = 2.0\theta_s. \quad (4)$$

The closest spacing between the reuse-beam edges,  $\theta_r$ , determines the achievable  $C/I$ , and is given by  $\theta_r = \theta_c - \theta_0$  (see Figure 2a). An important design parameter of the antenna is the feed size. The optimal feed size that gives the required beam spacing of  $\theta_s$  is given by

$$d_m^{3,4} = \theta_c^{3,4} / S_F. \quad (5)$$

The above equation assumes maximum diameter,  $d_m$ , of the circular horns such that adjacent feeds from the same reflector are touching each other. The parameter  $S_F$  in Equation (5) is the scan factor, which is defined as the ratio of the electrical scan angle of the beam to the physical displacement of the feed from the focal point. The scan factor is related to the reflector geometry shown in Figure 2b by

$$S_F = \frac{1 + X \left( \frac{D}{4F} \right)^2}{1 + \left( \frac{D}{4F} \right)^2} \tan^{-1} \left[ \frac{1 + \cos \theta_2}{2F} \right], \quad (6)$$

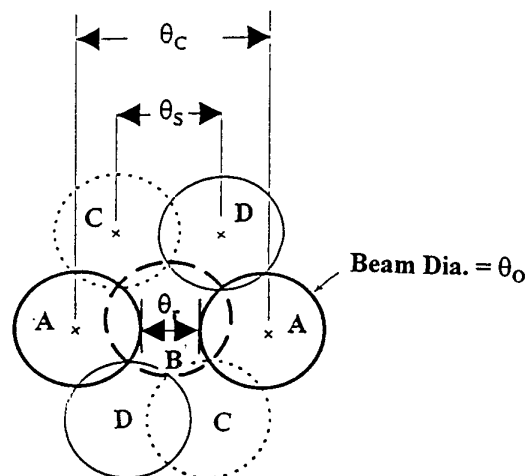


Figure 2a. The hexagonal-grid layout of a four-cell reuse MBA, showing the beam parameters.

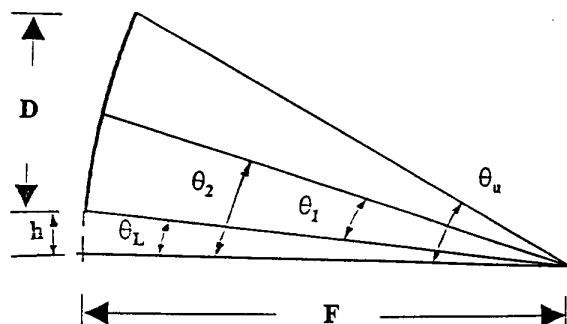


Figure 2b. The offset reflector geometry.

where

$$X = 0.30 \text{ for } T < 6 \\ = 0.36 \text{ for } T \geq 6, \quad (7)$$

and  $T$  is the feed illumination taper (+ve dB) on the edge of the reflector. The angular parameters of the offset reflector shown in Fig. 2b are given by

$$\theta_{1,2} = \frac{1}{2} \left\{ \tan^{-1} \left[ \frac{D+h}{F - \frac{(D+h)^2}{4F}} \right] \mp \tan^{-1} \left[ \frac{h}{F - \frac{h^2}{4F}} \right] \right\}. \quad (8)$$

Using the Gaussian-beam model for the feed horn, the primary radiation pattern can be represented as

$$E(\theta) = \exp \left[ -A(\theta/\theta_b)^2 \right], \quad (9)$$

where  $\theta_b$  is the half 3-dB beamwidth of the horn, which is given by

$$\theta_b = C_1 \frac{\lambda}{d_m}. \quad (10)$$

The constant  $C_1$  is 35 for a Potter-type horn, and is 31 for the dominant  $TE_{11}$ -mode circular horn;  $\lambda$  is the wavelength; and  $d_m$  is the feed diameter. The constant  $A$  is obtained using the relationship

$$E(\theta_b) = 0.707 = \exp(-A), \quad (11)$$

which gives the value of  $A$  as 0.3467. The feed-illumination taper,  $T$ , at the reflector edge is given by

$$T = -20 \log_{10} [E(\theta_1)] \\ = -20 \log_{10} \left[ \exp \left\{ -0.3467 \left[ \theta_1 (d_m/\lambda) / C_1 \right]^2 \right\} \right]. \quad (12)$$

The secondary pattern half-power full beamwidth for an on-axis beam is given by

$$\theta_3(\delta=0) = (0.762T + 58.44) \frac{\lambda}{D}, \quad (13)$$

where  $D$  is the projected diameter of the offset reflector. The above equation is valid for feeds located close to the focal point of the reflector, and is modified to include the beam-broadening effect with scan as given by [3].

$$\theta_3(\delta) = \theta_3(0) \cdot 10^{0.05GL}, \quad (14)$$

where  $GL$  is the gain loss due to scan in dB, and is given by

$$GL = \frac{0.0015\delta^2}{\left[ (F/D_p)^2 + 0.02 \right]^2} + \frac{0.011\delta^2}{\left[ (F/D_p)^2 + 0.02 \right]}. \quad (15)$$

$\delta$  in Equations (13) to (15) is the number of beamwidths,  $\theta_3(0)$ , scanned from boresight; and  $D_p$  is the diameter of the parent paraboloid, which is given by  $D_p = 2(D+h)$ . Equation (15) is obtained by interpolating the results of Ruze [4] in a quadratic form. For dielectric or waveguide lenses satisfying the Abbe sine condition (the thin-lens approximation), the gain loss in dB [5] is given by  $GL = 0.07\delta$  instead of Equation (15); the feed size can be obtained from  $d_m = F \tan \theta_c^{3,4}$ ; and the illumination angle,  $\theta_1$ , is given by  $\theta_1 = \tan^{-1}(D/2F)$ . The minimum directivity occurs at the triple beam crossover, and the level at the triple crossover point is given by

$$B(\delta) = 3 \left[ \theta_0 / \theta_3(\delta) \right]^2, \quad (16)$$

where  $B(\delta)$  is the overlap in dB (+ve) below the peak directivity. The above equation for the beam-crossover level assumes a Gaussian secondary radiation pattern.

### 3.1 MBA performance analysis

The beam directivity and the co-polar isolation ( $C/I$ ) among the frequency-reused beams can be estimated using the following analysis. The minimum-coverage-area directivity in dBi is given by

$$D_0 = 10 \log_{10} \left[ \left( \frac{\pi D}{\lambda} \right)^2 \eta_f \right] - GL(\delta_m) - B(\delta_m). \quad (17)$$

The first term of the above equation represents the peak directivity for beams close to the antenna boresight, and the second term represents the loss in directivity due to scan for the worst-case beam at the edge of coverage. The third term in Equation (17) is the triple beam crossover level (+ve dB) below the peak directivity.  $\delta_m$  is the maximum scan ratio, defined as the ratio of the worst-case scan angle to the half-power beamwidth,  $\theta_3(0)$ . Equation (17) gives better predictions than those using gain-area-product (GAP) values. The GAP-based estimates do not take into account either the reflector size or the feed illumination. The variable  $\eta_f$  in Equation (17) is the antenna-feed efficiency value, which is approximately equal to the overall antenna efficiency, and is given by [6, 7]

$$\eta_f = 4 \cot^2(\theta_1/2) \left[ 1 - \cos^n(\theta_1/2) \right]^2 \frac{(n+1)}{n^2}. \quad (18)$$

Equation (18) includes the spillover efficiency, aperture efficiency, phase efficiency, and polarization efficiency, and can easily be factored out into these four sub-efficiencies, as shown in [6]. The feed pattern is assumed to be of the form  $\cos^n(\theta/2)$  in the above equation. The value of the variable  $n$  in Equation (18) is given by

$$n = \frac{-0.05T}{\log \left[ \cos(\theta_1/2) \right]}. \quad (19)$$

The maximum value of the feed efficiency  $\eta_f$  is about 0.81, and occurs for feed-taper value of  $T \cong 10$  dB. Figure 3 shows the computed plot of the antenna efficiency as a function of the illumina-

tion taper,  $T$ . The parameter of the curves is the half-subtended angle of the reflector. The results show that a smaller  $\theta_1$  (a larger  $F/D$ ) results in better performance for an optimally illuminated MBA.

### 3.2 C/I analysis

The co-polar isolation of the downlink antenna is defined as the ratio of the co-polar directivity of the beam of interest to the combined interference directivity, obtained by adding all the interferers (that use the same frequency as the beam of interest) in power over the beam of interest. Figure 4 shows the beam geometry for the  $C/I$  calculations. The worst-case  $C/I$  typically occurs at the edge of the beam of interest. The directivity of the beam,  $C_0$ , at the edge is given by

$$C_0 = 10 \log_{10} \left[ \left( \frac{\pi D}{\lambda} \right)^2 \eta_f \right] - GL(\delta_0) - B(\delta_0) \text{ dBi}, \quad (20)$$

where  $\delta_0$  is the number of beamwidths scanned from the antenna boresight for the beam  $C_0$ . The combined interference signal, due to  $N$  interferers onto the beam of interest, is given by

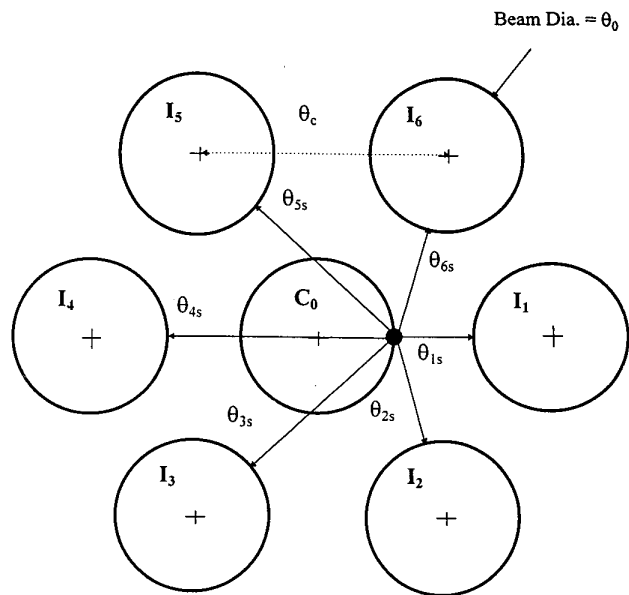


Figure 4. The beam geometry for  $C/I$  calculations.

$$\sum_{n=1}^N I_n = 10 \log_{10} \sum_{n=1}^N \left[ \left( \frac{\pi D}{\lambda} \right)^2 \eta_f 10^{-0.1GL(\delta_n)} 10^{-0.1B_n \left( \frac{\theta_{ns} + 0.5\theta_n}{0.5\theta_n} \right)^2} \right] \text{ dBi}. \quad (21)$$

$\theta_n$  in Equation (21) is the diameter of the  $n$ th interferer. It is assumed in Equations (20) and (21) that the antenna efficiency,  $\eta_f$ , does not change with scan. This is a valid assumption for moderate scans ( $\delta_m \leq 7$ ), and it is also valid for wide scans, provided that the feeds are located on a spherical cap with a radius  $R$  satisfying the equation  $R = F \sec^2(\theta_2/2)$ . The dominant interference is from the closest three interferers,  $I_1$ ,  $I_2$ , and  $I_6$  (see Figure 4), and is assumed to be from the skirt of the main-beam patterns of the interfering beams. This assumption is valid for most of the practical applications using either three-cell or four-cell frequency reuse. The effect of the sidelobes or coma-lobes due to scan is not considered here, as the levels are relatively low (typically around  $-24$  dB to  $-30$  dB relative to peak), and do not significantly impact the co-polar isolation values. It is to be noted that Equation (21) is valid for most of the practical values of  $F/D$  ratio (in the range 0.6 to 2.0).

The co-polar isolation in dB is given by

$$C_0 / \sum_{n=1}^N I_n = -GL(\delta_0) - B(\delta_0) - 10 \log_{10} \sum_{n=1}^N \left[ 10^{-0.1GL(\delta_n)} 10^{-0.1B_n \left( \frac{\theta_{ns} + 0.5\theta_n}{0.5\theta_n} \right)^2} \right]. \quad (22)$$

The above equation is in a general form, and is valid for nonuni-

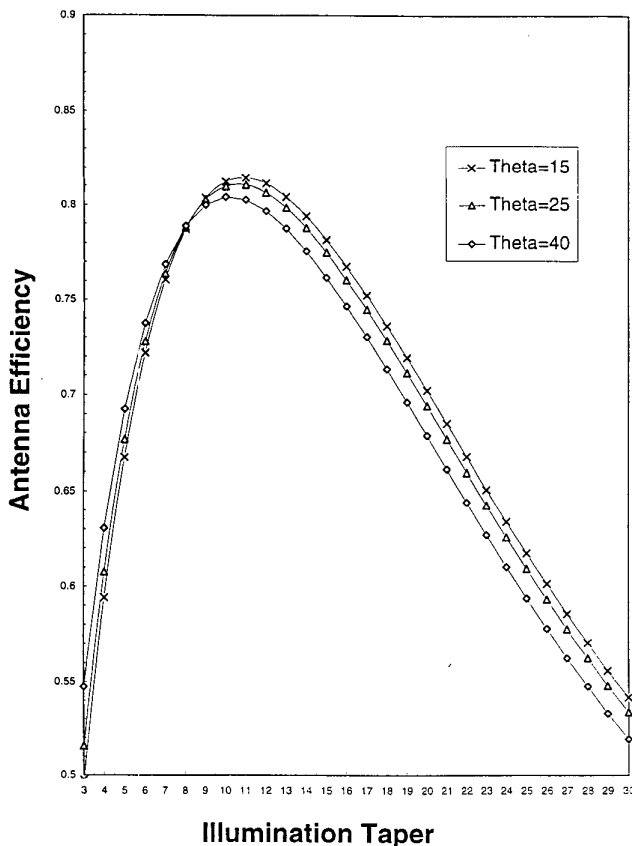


Figure 3. A plot of the antenna efficiency as a function of the feed taper ( $T$ ). The parameter of the curves is  $\theta_1$ .

form-size beams with nonuniform spacings. For a regular hexagonal-grid arrangement of the beams, as shown in Figure 4, the copolar isolation can be simplified by considering the closest six interferers, and is given approximately by

$$C_0 / \sum_{n=1}^N I_n = -B(\delta_0) - 10 \log_{10} \sum_{n=1}^6 10^{-0.1 B_n(\delta_n) \left( \frac{\theta_{ns} + 0.5\theta_0}{0.5\theta_0} \right)^2}, \quad (23)$$

where

$$\theta_{1s} = \theta_c - \theta_0 \quad (24)$$

$$\theta_{2s} = \theta_{6s} = \left[ \theta_c^2 + 0.25\theta_0^2 - 0.5\theta_c\theta_0 \right]^{0.5} - 0.5\theta_0 \quad (25)$$

$$\theta_{3s} = \theta_{5s} = \left[ \theta_c^2 + 0.25\theta_0^2 - 0.5\theta_c\theta_0 \right]^{0.5} - 0.5\theta_0 \quad (26)$$

$$\theta_{4s} = \theta_c. \quad (27)$$

### 3.3 Shaped-beam analysis

The analysis shown above for the MBAs can easily be extended to shaped beams. The minimum-coverage-area directivity of a shaped-beam antenna is typically estimated using the gain-area product (GAP). The GAP value varies from 13000 to 20000, depending on the size of the reflector and the extent of shaping. Obviously, this is not a good method, as the estimated directivity values can vary up to about 1.9 dB from the actual value, and they do not take into consideration either the reflector size or the feed illumination. Shaped beams can be produced either by using a paraboloidal reflector with multiple feeds, or by using a shaped reflector with a single feed. The analysis shown here is applicable to both the configurations. Using the MBA analysis shown in the previous section, the minimum-coverage-area directivity,  $D_{min}$ , can be estimated to be

$$D_{min} = 10 \log_{10} \left[ (\pi D / \lambda)^2 \eta_f \right] - M - GL(\delta_m) - 10 \log_{10} \left[ \frac{C_A}{(\pi/4)\theta_M^2} \right] \quad (28)$$

where  $C_A$  is the coverage area of the shaped beam in square degrees,  $\theta_M$  is the pencil-beam beamwidth at  $M$  dB below the peak directivity (a typical value of  $M$  is 4 for shaped beams), and  $GL(\delta_m)$  is the gain loss at the maximum scan angle of  $\delta_m$ . The maximum scan angle,  $\delta_m$ , is given by the coverage requirements, and depends on the actual coverage as seen by the satellite and the antenna boresight direction. The variable  $\theta_M$  is given by

$$\theta_M = \left[ \frac{M}{3} \right]^{0.5} \theta_3, \quad (29)$$

where  $\theta_3$  is the 3 dB full beamwidth as given by Equation (13).

## 4. Results

The simplified design and analysis results presented in the above sections are compared with those obtained from the rigorous Physical Optics analysis of the reflector antennas.

### 4.1 Multiple-beam antennas

The first example for comparison is an unscanned beam ( $\delta = 0$ ) of a 56-beam MBA with four reflectors and using a four-cell frequency reuse. The antenna parameters are  $D/\lambda = 106.9$ ,  $F/D = 1.324$ ,  $h/\lambda = 50.31$ ,  $\theta_0 = 0.545^\circ$ , and  $\theta_s = 0.472^\circ$ . Using the Gaussian-beam analysis given above, the design parameters are calculated as  $d_m/\lambda = 2.689$ ,  $T = 6.4$  dB,  $n = 53.5$ ,  $\eta_f = 0.741$ ,  $\theta_3 = 0.5923^\circ$ , and  $B = 2.54$  dB. The peak and edge-of-coverage (EOC) directivities, calculated using this analysis, are 49.22 dBi and 46.68 dBi, respectively. The computed values using the PO integration of surface currents on the reflector are 49.11 dBi (peak) and 46.54 dBi (EOC). The calculated and computed values for the co-polar isolation ( $C/I$ ) with six closest interferers are 12.0 dB and 12.5 dB, respectively.

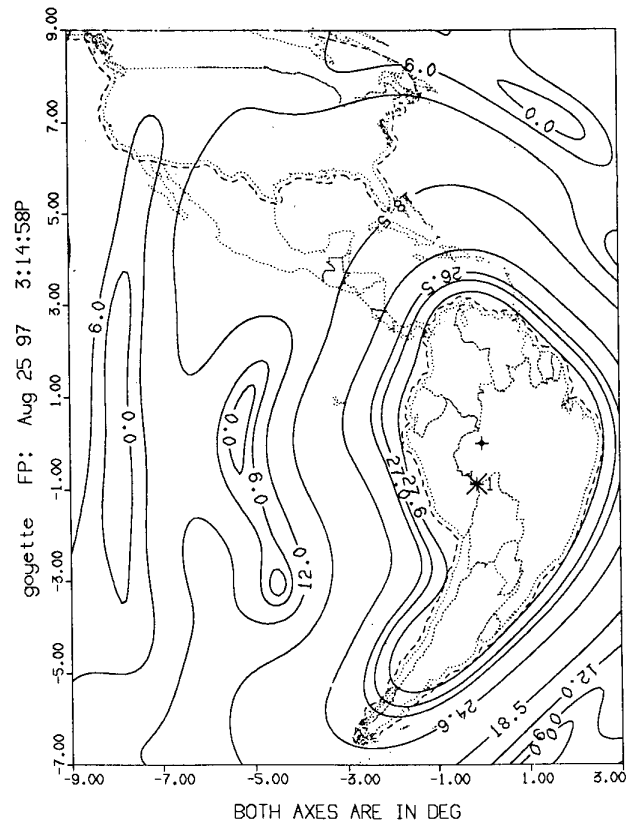


Figure 5. Computed directivity contours of a shaped-beam antenna using the PO method.

**Table 1: Comparison of the Analysis Results with Computations Based on the PO Software.**

Antenna Case	Peak Directivity, dBi		EOC Directivity, dBi		C/I, dB	
	Analysis	Computed	Analysis	Computed	Analysis	Computed
Case 1 (MBA)	49.22	49.11	46.68	46.54	12.00	12.50
Case 2 (MBA)	48.84	49.01	46.51	46.45	13.49	13.03
Case 3 (MBA)	46.97	46.70	42.33	41.92	21.20	19.80
Case 4 (Shaped Beam)	--	--	27.66	27.60	--	--
Case 5 (Shaped Beam)	--	--	21.33	21.70	--	--

The second example has the same antenna parameters as the first, except that the beam is scanned to  $1.666^\circ$  ( $\delta = 2.81$ ). The feed-design parameters are same as the first, and the beam parameters are calculated as  $\theta_3(\delta) = 0.6187^\circ$  and  $B = 2.33$  dB. The peak directivity, EOC directivity and C/I (with three interferers) values calculated using this analysis are 48.84 dBi, 46.51 dBi, and 13.49 dB, respectively, while the computed values using PO analysis are 49.01 dBi, 46.45 dBi, and 13.03 dB.

The last example uses a 24 beam MBA with four reflectors and four-cell frequency reuse. The antenna parameters are  $D/\lambda = 79.32$ ,  $F/D = 1.667$ ,  $h/\lambda = 39.66$ ,  $\theta_0 = 1.07^\circ$ , and  $\theta_s = 0.923^\circ$ . Design parameters are calculated as  $d_m/\lambda = 4.45$ ,  $T = 13$  dB,  $n = 159$ ,  $\eta_f = 0.802$ ,  $\theta_3 = 0.862^\circ$ , and  $B = 4.62$  dB. The calculated values for the peak directivity, EOC directivity, and C/I (with six interferers) are 46.97 dBi, 42.33 dBi, and 21.2 dB, while the respective values using the rigorous PO computations are 46.70 dBi, 41.92 dBi, and 19.8 dB. The calculated directivity values agree with computations within 0.4 dB, while the C/I values agree within 0.5 dB at the 13 dB level, and within 1.5 dB at the 20 dB level.

#### 4.2 Shaped beam antennas

The first example for shaped beams is a contoured beam covering South America. Antenna parameters for this case are  $D/\lambda = 28.45$ ,  $F/D = 0.824$ ,  $h/\lambda = 3.18$ ,  $T = 14$  dB,  $M = 4$  dB, and a coverage area  $C_A$  of 23.7 square degrees. The design parameters calculated are  $\theta_3 = 2.43^\circ$  and  $GL = 0.45$  dB. The calculated minimum-coverage-area directivity using the analysis shown is 27.66 dBi, while the computed value using the PO method (the coverage contours are shown in Figure 5) is 27.6 dBi.

Another example for shaped beams is a wide-area-coverage beam (semi-global), with antenna parameters of  $D/\lambda = 29$ ,  $F/D_p = 0.3125$ ,  $T = 13$  dB,  $M = 4$  dB, and  $C_A = 79.7$  square degrees. Design parameters calculated are  $GL = 1.57$  dB,  $\eta_f = 0.79$ , and  $\theta_3 = 2.383^\circ$  degrees. The calculated and PO-computed minimum directivity values are 21.33 dBi and 21.70 dBi, respectively. It is shown that the extension of the MBA analysis to shaped-beam antennas can predict the coverage directivity values within 0.4 dB of the PO computations. Comparison results for the multiple-beam antennas (shown in Section 4.1) and for shaped beams (shown in Section 4.2) are summarized in Table 1.

#### 5. Conclusion

Design and analysis methods for multiple-beam antennas shown in this paper can be employed for accurate design and quick analysis of MBA performance in terms of coverage directivity and co-polar isolation, without the need to compute the radiation patterns. This method is based on Gaussian-beam analysis of both primary and secondary patterns, and it gives performance-evaluation values very close to software predictions for moderate scans ( $\pm 7$  beamwidths). It is quite useful for initial design, design trades, and performance evaluation of MBAs. Extension of this method to shaped-beam antennas was also shown to predict performance close to software computations using PO integration of the surface currents.

#### 6. References

1. K. S. Rao et al., "Development of a 45 GHz Multiple-Beam Antenna for Military Satellite Communications," *IEEE Transactions on Antennas and Propagation*, **AP-43**, 10, October 1995, pp. 1036-1047.
2. K. S. Rao et al., "Multiple Beam Antenna Concepts for Satellite Communications," ANTEM Conference, Ottawa, Canada, August 1994.
3. K. S. Rao, "A Template for Shaped-Beam Satellite Antenna Patterns," *IEEE Transactions on Antennas and Propagation*, **AP-36**, 11, November 1988, pp. 1633-1637.
4. J. Ruze, "Lateral-Feed Displacement in a Paraboloid," *IEEE Transactions on Antennas and Propagation*, **AP-13**, September 1965, pp. 660-665.
5. K. K. Chan et al., "Triangular Ray-Tube Analysis of Dielectric Lens Antennas," *IEEE Transactions on Antennas and Propagation*, **AP-45**, 8, August 1997, pp. 1277-1285.
6. P. S. Kildal, "Factorization of the Feed Efficiency of Paraboloids and Cassegrain Antennas," *IEEE Transactions on Antennas and Propagation*, **AP-33**, 8, August 1995, pp. 903-908.
7. K. S. Rao and P. S. Kildal, "A Study of the Diffraction and Blockage Effects on the Efficiency of the Cassegrain Antenna," *Canadian Electrical Engineering Journal*, **9**, 1, January 1984, pp. 10-15.

## Introducing Feature Article Author



**Sudhakar K. Rao** received the BTech degree in electronics engineering from the Regional Engineering College, Warangal, India, in 1974, the MTech degree in Radar Systems Engineering from the Indian Institute of Technology, Kharagpur, in 1976, and the PhD degree in electrical engineering from the Indian Institute of Technology, Madras, in 1980.

From 1976 to 1977, he worked as a Technical Officer at the Electronics Corporation of India Limited (ECIL) and was involved with the design and test of LOS and TROPO communication antennas. He was a Research Assistant at the Indian Institute of Technology, Madras, during 1977 to 1980, and worked on the application of GTD techniques for horn antennas. He worked as a Senior Scientific Officer at the Electronics and Radar Development Establishment (LRDE), Bangalore, from 1980 to 1981, and was involved with the design and analysis of phased-array radar antennas. From 1981 to 1982, he worked at the University of Trondheim, Norway, on Earth-station antennas, and had a post-doctoral

fellowship from the Royal Norwegian Council for Scientific and Industrial Research (NTNF). He was a Research Associate at the University of Manitoba, Winnipeg, Canada, during 1982-1983, and worked on low-sidelobe antennas. From 1983 to 1996, he worked with Spar Aerospace Limited, Ste-Anne-de-Bellevue, Quebec, Canada, in the Satellite Systems Division. There, he worked on commercial satellite payloads, mobile personal communication antennas, agile beam antennas at EHF, and active antennas. He is currently working with Hughes Space and Communications, Los Angeles, California, as a Chief Scientist. His current research interests are reconfigurable payloads and multiple-beam antennas for both commercial and military applications.

Dr. Rao is a Senior Member of the IEEE, and has published over 70 papers in technical journals and conferences in the area of microwave antennas. He has filed for 10 patents. His work on the modeling of satellite-antenna patterns was adopted by the CCIR in 1992. ☞

---

## New IEEE Video Helps to Prepare Engineers for PE Exam

The IEEE has released "P.E. Review: Electronics," a video tutorial intended to help prepare engineers to take the Electronics portion of the Professional Engineering (PE) Licensing examination, to be given in October, 1999, or April, 2000. "P.E. Review: Electronics" focuses on concepts required to analyze and design complex circuits, and provides valuable hints on maximizing test scores. State licensing boards use examinations prepared by the National Council of Examiners for Engineering and Surveying (NCEES). Expanding on the sample problems put forth in the NCEES's "Principles and Practice of Engineering (PE)," this video tutorial covers the following topics:

- Bipolar junction transistors (BJTs)
- Field-effect transistors (FETs)
- Switching power supplies
- Operational amplifiers
- Frequency response

and much more.

The presenters on the video are Dr. Martin S. Roden and Dr. Sidney Soclof, who together have 65 years of experience, including courses presented through instructional-television networks. Drs. Roden and Soclof are both professional engineers and university professors.

The running time of the video is two hours and 15 minutes. The IEEE order number is HV7044-QVE. The list price is \$199.00; the IEEE member price is \$125.00. The video can be ordered from IEEE Customer Service, 445 Hoes Lane, PO Box 1331, Piscataway, NJ 08855-1331, USA; Tel: +1 (800) 678-4333; E-mail: [customer-service@ieee.org](mailto:customer-service@ieee.org). Prospective purchasers should contact the IEEE before placing an order. More information is available on the Web at <http://www.ieee.org/eab>. For more information on this video tutorial, those interested can also contact Patty Mickus, IEEE Media Producer: E-mail: [p.mickus@ieee.org](mailto:p.mickus@ieee.org). More about PE licensure is available at the NCEES Web site at [www.ncees.org](http://www.ncees.org).

[Information for the above item was taken from an IEEE press release.]